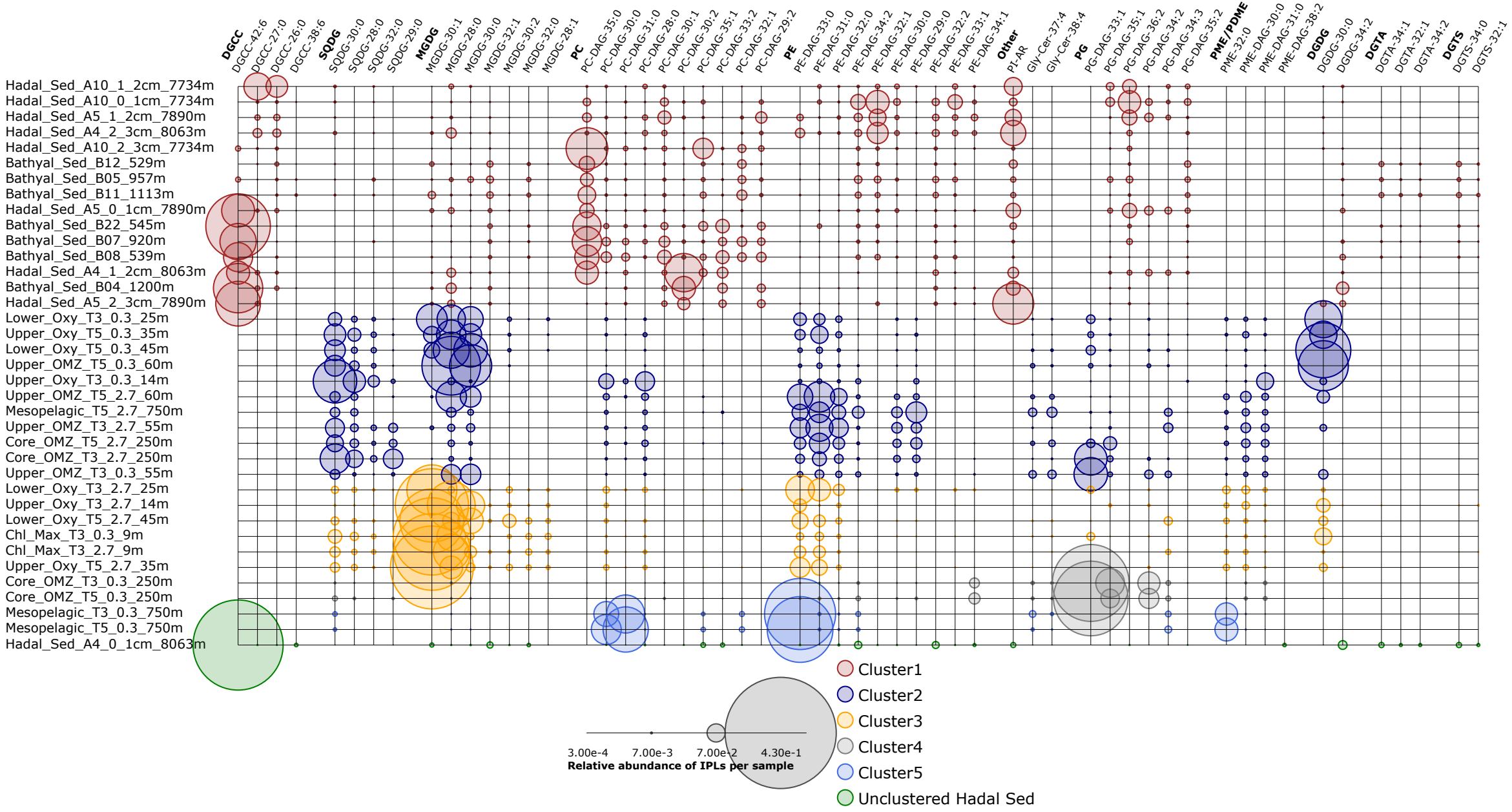
DGCC
DGCC-42:6
DGCC-27:0
DGCC-26:0
DGCC-38:6
SQDG
SQDG-30:0
SQDG-28:0
SQDG-32:0
SQDG-29:0
MGDG
MGDG-30:1
MGDG-28:0
MGDG-30:0
MGDG-32:1
MGDG-30:2
MGDG-32:0
MGDG-28:1
PC
PC-DAG-35:0
PC-DAG-30:0
PC-DAG-31:0
PC-DAG-28:0
PC-DAG-30:1
PC-DAG-30:2
PC-DAG-35:1
PC-DAG-33:2
PC-DAG-32:1
PC-DAG-29:2
PE
PE-DAG-33:0
PE-DAG-31:0
PE-DAG-32:0
PE-DAG-34:2
PE-DAG-32:1
PE-DAG-30:0
PE-DAG-29:0
PE-DAG-32:2
PE-DAG-33:1
PE-DAG-34:1
Other
PI-AR
Gly-Cer-37:4
Gly-Cer-38:4
PG
PG-DAG-33:1
PG-DAG-35:1
PG-DAG-36:2
PG-DAG-34:2
PG-DAG-34:3
PG-DAG-35:2
PME/PDME
PME-32:0
PME-DAG-30:0
PME-DAG-31:0
PME-DAG-38:2
DGDG
DGDG-30:0
DGDG-34:2
DGTA
DGTA-34:1
DGTA-32:1
DGTA-34:2
DGTS
DGTS-34:0
DGTS-32:1
Hadal_Sed_A10_1_2cm_7734m
Hadal_Sed_A10_0_1cm_7734m
Hadal_Sed_A5_1_2cm_7890m
Hadal_Sed_A4_2_3cm_8063m
Hadal_Sed_A10_2_3cm_7734m
Bathyal_Sed_B12_529m
Bathyal_Sed_B05_957m
Bathyal_Sed_B11_1113m
Hadal_Sed_A5_0_1cm_7890m
Bathyal_Sed_B22_545m
Bathyal_Sed_B07_920m
Bathyal_Sed_B08_539m
Hadal_Sed_A4_1_2cm_8063m
Bathyal_Sed_B04_1200m
Hadal_Sed_A5_2_3cm_7890m
Lower_Oxy_T3_0.3_25m
Upper_Oxy_T5_0.3_35m
Lower_Oxy_T5_0.3_45m
Upper_OMZ_T5_0.3_60m
Upper_Oxy_T3_0.3_14m
Upper_OMZ_T5_2.7_60m
Mesopelagic_T5_2.7_750m
Upper_OMZ_T3_2.7_55m
Core_OMZ_T5_2.7_250m
Core_OMZ_T3_2.7_250m
Upper_OMZ_T3_0.3_55m
Lower_Oxy_T3_2.7_25m
Upper_Oxy_T3_2.7_14m
Lower_Oxy_T5_2.7_45m
Chl_Max_T3_0.3_9m
Chl_Max_T3_2.7_9m
Upper_Oxy_T5_2.7_35m
Core_OMZ_T3_0.3_250m
Core_OMZ_T5_0.3_250m
Mesopelagic_T3_0.3_750m
Mesopelagic_T5_0.3_750m
Hadal_Sed_A4_0_1cm_8063m
3.00e-4
7.00e-3
7.00e-2
4.30e-1
Relative abundance of IPLs per sample
Cluster1
Cluster2
Cluster3
Cluster4
Cluster5
Unclustered Hadal Sed